Anadolu Üniversitesi Bilim ve Teknoloji Dergisi A- Uygulamalı Bilimler ve Mühendislik
Anadolu University Journal of Science and Technology A- Applied Sciences and Engineering

2017 - Volume: 18 Number: 5
Page: 1077 - 1088
DOI: 10.18038/aubtda.323679
Received: 25 June 2017 Revised: 16 October 2017 Accepted: 17 October 2017

MECHANICAL BEHAVIOR OF PRESTRESSED VISCOELASTIC ADHESIVE AREAS UNDER COMBINED LOADINGS

Halil M. ENGİNSOY [1,*], Osman ASİ [1]

[1] Department of Mechanical Engineering, Faculty of Engineering, Uşak University, Uşak, Turkey

ABSTRACT

In this study, the mechanical behaviors of the adhesive tape VHB 4950 elastomeric material are experimentally and numerically investigated. The VHB 4950 adhesive tape, which has viscoelastic behavior, is an element of acrylic polymer group and under different pre-stress conditions and complex forces (due to the different geometry of the designed test specimen). In experimental studies, the loading-unloading cyclic test, that is a kind of different standardized test for the mechanical characterization of viscoelastic material, is applied which give the most suitable convergent optimization parameters for the finite element model. Different material models are also investigated by using the data obtained from loading-unloading cyclic test results in all numerical models. According to the experimental results, the most suitable material parameters are determined with the Abaqus Parallel Rheological Framework Model (PRF) for the 4 Yeoh Networks with Bergstrom-Boyce Flow model which is created in the Mcalibration software for finite element analysis. By using these material parameters, the finite element analysis is performed by Abaqus software as three dimension non-linear viscoelastic. The finite element analysis results show good correlation to the Force (N)-Displacement (mm) experimental data for the maximum load-carrying capacity of the structural specimens.

Keywords: Viscoelasticity; PRF Modelling; Simulation; VHB 4950

1. INTRODUCTION

In the last century, experimental and numerical investigations on the mechanical behavior of elastomeric materials have been studied [1]. Acrylic polymers, which are elastomeric materials for industrial applications (automotive, marine, aviation and biomechanics etc.), have widely used as adhesives. Viscoelastic properties need to be defined in order to precisely determine the mechanical behavior under various loadings where acrylic adhesive is used [2]. Viscoelastic mechanical behaviors vary according to their chemical composition, and different mechanical behaviors are observed under different loads [3]. Acrylic polymers are also used for electro-mechanical couplings. Many researches have been widely carried out electro active polymer actuators in their studies [4-8]. In addition, the behavior of the load carrying capacity in the large strains and dynamic loads for a large number of structures is also investigated [9]. There are limited previously conducted studies to investigate the background of our present study [1-9]. The main differences of our research from the others are as follows: Systematically applied combined loads (due to the dimensional ratio of the test specimens) and different pre-stresses effects on the structures are performed experimentally and numerically.

VHB 4950 (3M ™), that has nonlinear viscoelastic behavior, is an important tool for different applications. For this reason, there are different experimental tests standardized in the literature for the identification of mechanical behaviors [8]. Within the scope of this study: single-step relaxation tests, multi-step relaxation tests, monotonic tests, and loading-unloading cyclic tests are performed under different strain rates and different deformation levels. These tests are used to obtain a detailed mechanical characterization of the viscoelastic material. However, in this study, we present loading - unloading cyclic tests which are used to obtain the best suitable condition with the numerical model.

*Corresponding Author: murat.enginsoy@usak.edu.tr

Acrylic polymers exhibit both elastic and viscous material behaviors at the same time. For this reason, they should be modeled and analyzed precisely with various simulation tools before they are used in application areas. In the literature, the modeling of the elastic behavior is based on Neo-Hooke, Mooney-Rivlin, Ogden, Yeoh etc. On the other hand, Bergstrom-Boyce Flow, Hyperbolic-Sine Flow, Power-Law Flow and Power-Law Strain Flow etc. are used for the modeling of viscoelastic behaviors. The viscoelastic energy dissipation can be modeled more accurately and accurately with the Parallel Rheological Framework model (PRF) for determining non-linear viscoelastic behaviors [10]. Thus, the results of numerical studies data are determined to provide the best fit with the result obtained from experimental studies. In this study, Yeoh model is used in hyperelastic modeling of elastic behavior and the Bergstrom-Boyce model is used for modeling viscoelastic behaviors. The data obtained from the loading-unloading cyclic tests are modeled in material concept with the Abaqus Parallel Rheological Framework Model for 4 Yeoh Networks with Bergstrom-Boyce Flow in the Mcalibration software database. By including them in the pre-stresses of different values determined within the scope of our study, the structural analysis with the finite element software Abaqus is performed as a whole.

This paper is organized as follows: In section 2, the mechanical behaviors of the constituents of the test specimens designed for the purposes are determined by appropriate standard tests. The application of different pre-stresses on structural assemblies to provide composite loads is explained. Then the methods applied in three dimensions and non-linear numerical modeling are expressed. In section 3, the data obtained as results of experimental and numerical studies are shown comparatively. In section 4, the results of the study are evaluated by the effects of variable parameters such as pre-stresses, different combined loading values and different amounts of adhesion surfaces on the maximum load carrying capacity.

2. MATERIALS AND METHODS

2.1. Specimen

Composite material specimens used for the structural loadings are manufactured from unidirectional E-glass reinforced and epoxy matrix using hand lay-up technique at Izoreel Company. The laminated E-glass/epoxy composite has 3 mm thickness. Illustration of the dimensional parameters of the specimens determined as research and the structural composition is given in Figure 1. In addition, the composite specimens are cut with water jet to make dimensional changes as given in Table 1.

Table 1. Geometric parameters of specimen design

<table>
<tr><td colspan="2" rowspan="3">Dimensional Ratio</td><td colspan="4">Dimensional Ratio</td><td rowspan="3">Dimension (mm)</td></tr>
<tr><td colspan="4">c/a</td></tr>
<tr><td>0,4</td><td>0,5</td><td>0,6</td><td>0,7</td></tr>
<tr><td colspan="2"></td><td>16</td><td>20</td><td>24</td><td>28</td><td>c</td></tr>
<tr><td rowspan="4">d/c</td><td>0,4</td><td>6,4</td><td>8</td><td>9,6</td><td>11,2</td><td rowspan="4">d</td></tr>
<tr><td>0,5</td><td>8</td><td>10</td><td>12</td><td>14</td></tr>
<tr><td>0,6</td><td>9,6</td><td>12</td><td>14,4</td><td>16,8</td></tr>
<tr><td>0,7</td><td>11,2</td><td>14</td><td>16,8</td><td>19,6</td></tr>
<tr><td rowspan="3">b/a</td><td>0,8</td><td colspan="4">32</td><td rowspan="3">b</td></tr>
<tr><td>1</td><td colspan="4">40</td></tr>
<tr><td>1,2</td><td colspan="4">48</td></tr>
<tr><td colspan="7">a=40 mm (constant dimension for every specimen)</td></tr>
</table>

Table 1 shows the systematic variation of the dimension ratios of the test specimen design parametrically. The geometric locations of the parameters representing the sample sizes are shown in

Figure 1. The dimensions of the specimens are determined using the values obtained from the proportional changes. In Fig. 1, the areas, showed as adhesive area, are used in the dimensions of 1.1 mm ± 10% (3M ™) VHB 4950 viscoelastic adhesive tapes designed to fit. Prior to bonding, pre-cleaning with (3M ™) Primer 94 is applied to the surface to be treated in order to achieve maximum adhesion performance.

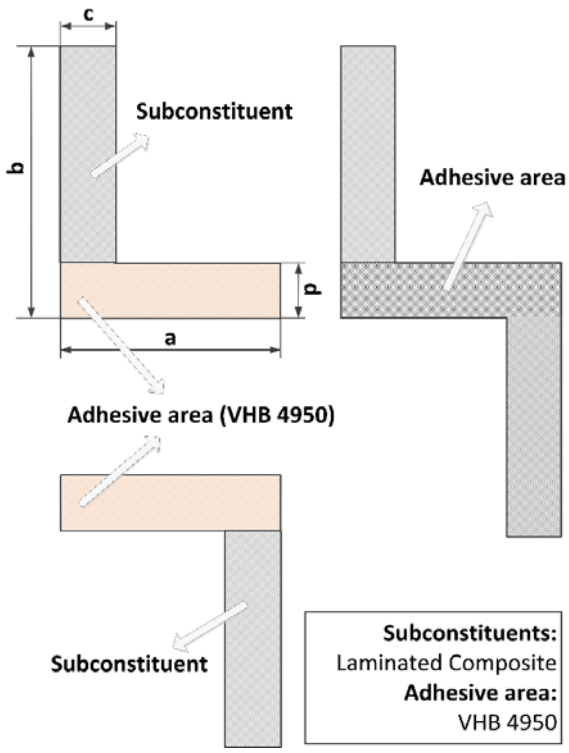

Figure 1. General schematic drawing for designed combined loading specimens.

2.2. Experimental Tests of Constituents

VHB 4950 viscoelastic adhesive tape is manufactured by 3M^{TM}. Some mechanical properties of viscoelastic adhesive tape VHB 4950 (given by the manufacturer) are given in Table 2 and this data are used in the finite element model.

Table 2. The mechanical properties of VHB 4950 [26].

VHB 4950 Properties	Value	Unit	Test Standard
90° Peel Adhesion	44	N/cm	ASTM D3330
Normal Tensile	970	kPa	ASTM D897
Dynamic Overlap Shear	550	kPa	ASTM D1002

All tests are carried out at 10:1 aspect ratio at constant ambient temperature and without deformation of the tape so that the viscoelastic behaviors of the VHB 4950 adhesive tape could be determined completely [11]. For loading-unloading cyclic tests, viscoelastic tape specimen geometry is used in the dimensions of 100 mm x 10 mm. All of the viscoelastic tests are carried out under the hand-controlled set-up conditions with the Zwick (Z010) machine.

In order to determine the rate-dependent properties of the most important mechanical behaviors of the polymeric viscoelastic material, the loading-unloading cyclic tests have a major consideration [12-20]. Within the scope of the study, the loading-unloading tests are repeated at least five times for each sample that prepared under different strain rates (2 different) and different stretch levels (4 different). The graphs of mean values of the obtained data are given in Figure 2. Loading-unloading cyclic tests are applied under four different deformations; 50% deformation (stretch level 1.5) given in Figure 2a, 100% deformation (stretch level 2.0) given in Figure 2b, 150% deformation (stretch level 2.5) given in Figure 2c, 200% deformation (Stretch level 3.0) given in Figure 2d. Each deformation is applied at two different strain rates such as under 0.01 s^{-1} and 0.05 s^{-1} strain rates. It is observed that the most accurate results for determining behavior of the material dissipation with various tests made on the viscous material at the determined strain rates are 0.01 s^{-1} and 0.05 s^{-1}. Therefore, these strain rate values are applied in each test. The data obtained in this context are used during the determination of hyperelastic and viscous material parameters during creation of the finite element model, as mentioned in section 2.4.

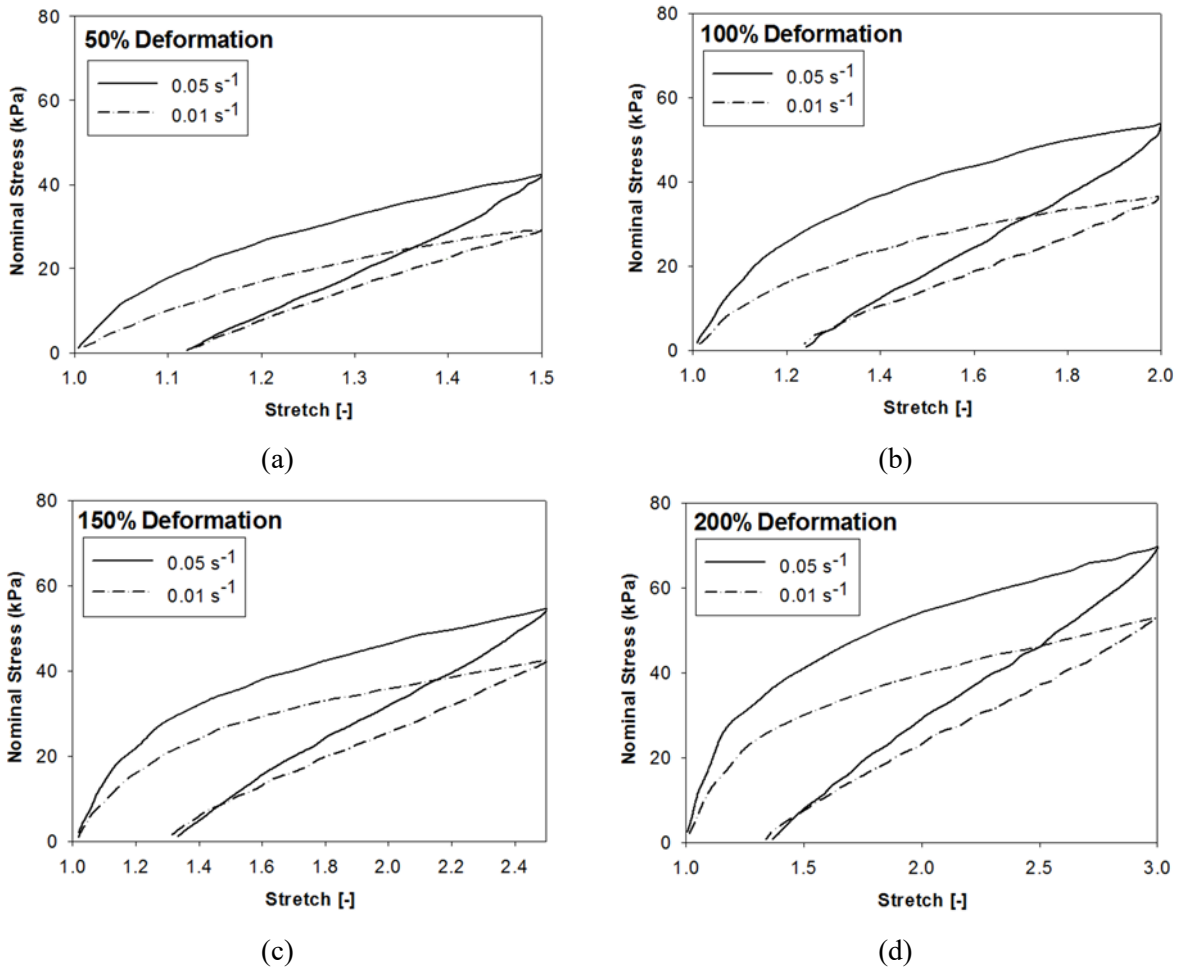

Figure 2. Loading – unloading tests with different strain rates (0.05 s^{-1} and 0.01 s^{-1}) and different (a) 50% deformation, (b) 100% deformation, (c) 150% deformation, (d) 200% deformation conditions

Mechanical properties of the unidirectional reinforced E-glass and epoxy laminated composites are determined using ASTM D3846-79 - ASTM D3410 - ASTM D3039-76 standards. The average results are tabulated in Table 3. This data is used in the finite element model.

Table 3. The mechanical properties of laminated composite plate.

Properties	**Value**	**Properties**	**Value**
Longitudinal modulus (E_1)	42.5 GPa	Longitudinal compressive strength (X_c)	300 MPa
Transverse modulus (E_2)	11.8 GPa	Transverse compressive strength (Y_c)	78 MPa
In-plane shear modulus (G_{12})	3.65 GPa	In-plane shear strength (S)	90 MPa
Major poisson's ratio (υ_{12})	0.23	Interlaminar shear strength (S_i)	65 MPa
Longitudinal tensile strength (X_t)	770 MPa	Fiber volume fraction (V_f)	58%
Transverse tensile strength (Y_t)	110 MPa	Number of layers	16

2.3. Experimental tests of Structures

In the previous section, the mechanical behaviors of the components of the structure (as shown in Figure 1) are experimentally determined. In this section, the application of prestressing on structural joining, which is one of the basic aims of this study, is given. The specimens are cut from laminated composite plates and assembled on the adhesion area specified by VHB 4950. In Figure 3, a computer-controlled hydraulic press is shown to unite and apply prestresses continuously for 72 hours at different values. The applied prestress values are 10 N/mm^2 (Group1:G1), 20 N/mm^2 (Group2: G2), 40N/mm^2 (Group3:G3) and 80 N/mm^2 (Group4:G4). Each prestress group comes to the front of the specimen nomenclature, by naming all the samples as given in brackets above. The specimen nomenclatures for each specimen, that is designed according to the parameters given in Table 1, is made by taking the c dimension as the base dimension. For example; 16a1 specimen nomenclature means: c=16mm – d=6.4mm – b=32mm and indicates that a dimension is a constant value of 40 mm, valid for all specimens. Then 16a1 specimen joined under 10 N/mm^2 prestress is named G1-16a1. Furthermore, detailed dimensional properties of maximum load carrying capacity specimens are given in Table 7.

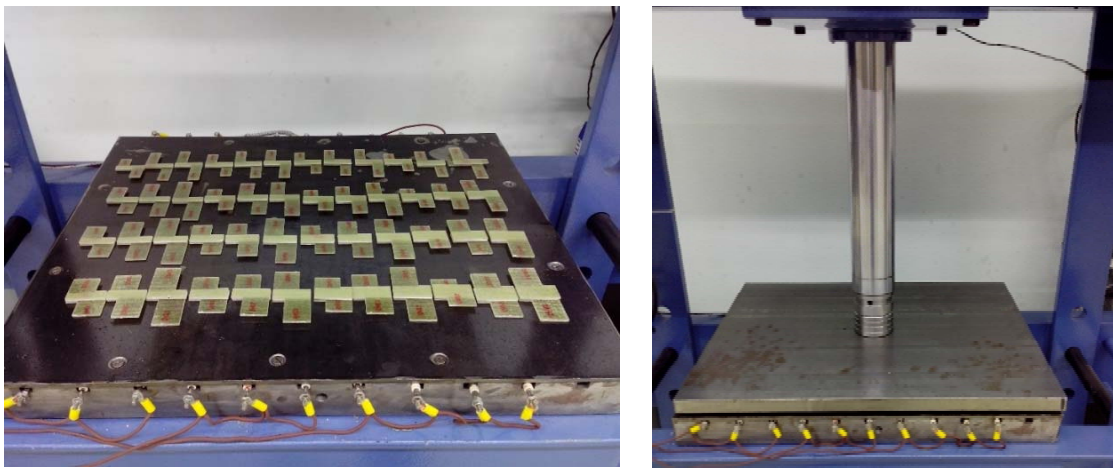

(a) **(b)**

Figure 3. A computer controlled hydraulic press unit: (a) general view of assembled structural specimens to be prestressed, (b) application of prestressing on structural specimens

The tensile tests are applied at constant 1mm/min on the combined structural specimens under different pre-stress values. During tensile tests, bending and torsion moments due to the design of the joined structures are also effected on the adhesion surface. Thus, the force (N) - displacement (mm) behaviors of the VHB 4950 tape, which is the adhesion surface, are investigated as a result of maximum stress under prestressed and combined loads. In Figure 4, the specimen is under the tensile test, (a) end of test and (b) finite element analysis result (as an example). Also, the viscoelastic tape used in the adhesive area has undergone separation of the first end portion of the damage as a result of applied combined

loads; and as the last damage, it is found to leave the whole surface. Similarly, the finite element analysis has been observed that this situation is confirmed.

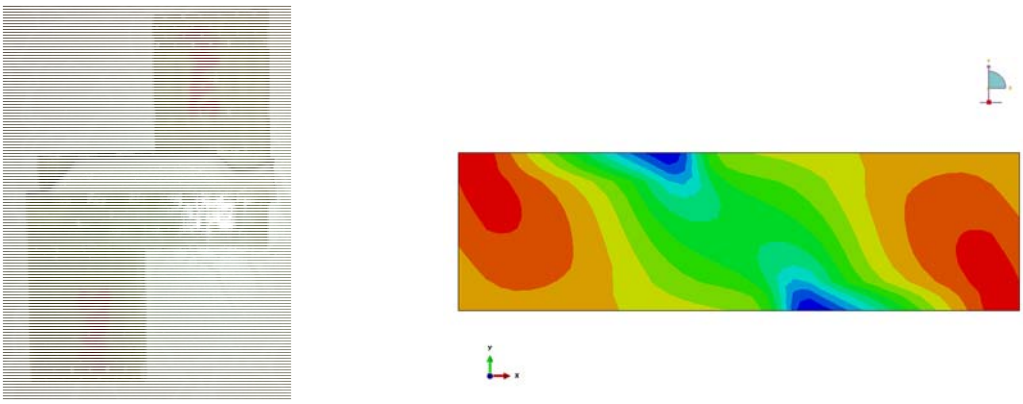

(a) **(b)**

Figure 4. The specimen under tensile test, (a) test result and (b) finite element analysis stress distribution result for VHB 4950 tape (G1-20a4 specimen).

2.4. Numerical Modelling

The loading-unloading cyclic test data given in section 2.2 is used to construct a three-dimensional nonlinear finite element model. The test data are used to determine the optimum material parameters to be used in the finite element model with various material models included in the Mcalibration software. In the Mcalibration software, the most suitable convergent material model is investigated with the experiment data. Detailed information on all of the material models given in Table 4 can be found in Ref. [21]. It is determined that the optimum material parameters are obtained under the conditions of 50% deformation with 0.01 s^{-1} strain rate in the research process. In Table 4, model calibration results for different material models under 10% error values are given.

Table 4. Calibration results from different material models under 10% error for VHB 4950. (Under 50% deformation with 0.01 s^{-1} strain rate condition)

Abaqus Material Model	**Error in Model Calibration (%)**
Hyperelastic-Mullins-Mooney-Rivlin	8.9844
Hyperelastic-Mullins-Ogden	8.4436
Hyperelastic-Mullins-Yeoh	7.0855
PRF Model: 3 Yeoh Networks with Bergstrom-Boyce Flow	4.4530
PRF Model: 4 Yeoh Networks with Hyperbolic-Sine Flow	4.3408
PRF Model: 4 Yeoh Networks with Power-Law Flow	3.0458
PRF Model: 4 Yeoh Networks with Power-Law Strain Flow	2.7462
PRF Model: 4 Yeoh Networks with Bergstrom-Boyce Flow	2.4284

The most accurate results in modeling the time dependent-rate mechanical response characteristic of the model, shown in detail in Figure 2, (to be valid for all material models given in Table 4) are found to give the nominal stress values obtained under 50% deformation (stretch level 1.5) and 0.01 s^{-1} strain rate conditions. In Figure 5, an illustration of the Parallel Rheological Framework (PRF) model, which is used numerically in material modeling, is given.

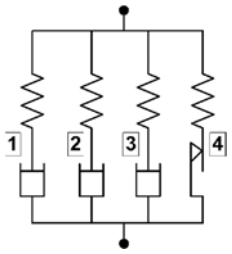

Figure 5. Illustration of Parallel Rheological Framework (PRF) Model.

The values showing the errors in the Abaqus Parallel Rheological Framework Model 4 Yeoh Networks with Bergstrom-Boyce Flow model calibration that are used under these conditions are given in Table 5.

Table 5. Calibrations results from different strain and different stretch rates for VHB 4950

.

Deformation (%)	Stretch (λ)	Strain Rates (s^{-1})	Error in Model Calibration (%)
50	1.5	0.01	2.4284
		0.05	3.7999
100	2	0.01	15.0709
		0.05	10.4222
150	2.5	0.01	24.1359
		0.05	21.0404
200	3	0.01	32.6812
		0.05	32.4769

The Parallel Rheological Framework (PRF) Abaqus models, which are included in the Mcalibration software, provide more realistic results in material modeling for finite element analysis [22-23]. PRF models are based on the principle of superposition in parallel modeling of finite strain hyperelastic and viscoelastic networks in the model of non-linear viscoelastic behaviors [24]. The PRF model for Yeoh Networks with Bergstrom-Boyce model in Mcalibration is a model used for optimization of highly non-linear elastomeric materials parameters. The most consistent result with the experimental data obtained for the VHB 4950 is also shown in this model. The optimum material parameters obtained as a result of the calibration are given in Table 6.

The Yeoh model (network 4) in PRF is a model of hyperelastic material. The Yeoh model is a useful model for different loading modes [21] and is given below for Cauchy stress with Equation 1.

$$\boldsymbol{\sigma} = \frac{2}{J}\{C_{10} + 2C_{20}(I_1^* - 3) + 3C_{30}(I_1^* - 3)^2\}dev[\mathbf{b}^*] + \kappa(\mathrm{J} - 1)\mathbf{I} \tag{1}$$

where hyperelastic (equilibrium) response network 4 parameters:

C_{10}: First Yeoh, C_{20}: Second Yeoh, C_{30}: Third Yeoh parameters; κ (kappa): Bulk modulus of the Yeoh model; σ: Cauchy stress and $\mathrm{J} = \det(\mathbf{F})$ and $\mathbf{b}^* = \mathrm{J}^{\frac{-2}{3}}\boldsymbol{F}\boldsymbol{F}^{\mathrm{T}}$: left distortional left Cauchy-Green tensor.

Bergstrom - Boyce (BB) model (network 1, 2, 3), another model in the PRF, consists of two networks connected in parallel to each other in the molecular level. It shows the initial network equilibrium behavior and other network time-dependent deviation from equilibrium state. The BB model expresses the rate of change of the viscoelastic flow as a function of the applied stress and deformation state [25]. BB model is given with Equation 2.

$$\dot{\gamma}^p = [\lambda_L - 1 + \xi]^C . \left(\frac{\tau}{\tau_{base}}\right)^m \tag{2}$$

where, $\dot{\gamma}^p$: flow rate; λ_L: chain stretch; ξ: Strain adjustment factor; C: Strain power exponent; τ: applied shear stress; τ_{base}: Flow resistance stress; m: Shear flow exponent.

The model parameters of the viscoelastic VHB 4950 tape given in Table 2 and Table 6 are used in finite element analysis with commercial software Abaqus. In the modeling process, the parameters obtained in the Mcalibration software are provided via the Abaqus input file for transfer to the finite element analysis software. Laminated composite plates providing combined loads on the viscoelastic tape are modeled according to the parameters as given in Table 3. The C3D8R (an 8-node linear brick, reduced integration) element type is used for the mesh processing of the viscoelastic material model.

Table 6. Loading-unloading cyclic test with Abaqus PRF Model for 4 Yeoh Networks with Bergstrom-Boyce Flow model parameters (50% deformation – 0.01 s^{-1})

Network 4 Hyperelastic		**Network 1**		**Network 2**		**Network 3**	
		S_1	0.721729	**S_2**	0.00026191	**S_3**	0.206511
C_{10}	7.10882	**τ_{base1}**	6.78044	**τ_{base2}**	12.4017	**τ_{base3}**	53.9199
C_{20}	-1.4984	**m_1**	11.4311	**m_2**	11.1661	**m_3**	14.2368
C_{30}	0.072382	**C_1**	-0.298672	**C_2**	-0.146765	**C_3**	-0.0482543
κ	2000	**E_1**	0.001	**E_2**	0.001	**E_3**	0.001

where *n* is Network 1, 2 and 3 index parameters (*n*=1, *n*=2, *n*=3); S_n: Scale factor is compared to each Network (n); E_n: Strain offset factor.

3. RESULTS AND DISCUSSION

In this study, maximum load carrying capacities VHB 4950 viscoelastic tape under combined loads are investigated experimentally and numerically. The viscoelastic tape under different prestressed is modeled by using the optimum material parameters obtained with the Abaqus Parallel Rheological Framework Model for 4 Yeoh Networks with Bergstrom-Boyce Flow model.

The experimental and finite element analysis results of the specimens with maximum load carrying capacity are classified according to those having the same c dimension. Their investigations are also given below in detail.

- In Figure 6, the experimental and finite element analysis results of the specimens, carrying maximum load of the 16a series, are given comparatively. In general, the maximum values for load carrying capacities are in the range of 250 N (± 25 N) and 5 mm (± 0.5 mm). The specimen G1-16a11 is determined to have the maximum load carrying capacity. For other specimens it is determined that the maximum load carrying capacity decreases as the amount of prestress increases.

- In Figure 7, the experimental and finite element analysis results of the specimens, carrying maximum load of the 20a series, are given comparatively. In general, the maximum approximate values for the load carrying capacities are around 435 N and 4 mm for the G1-20a11 specimen. In the other specimens, it is determined that the maximum load carrying capacity decreases as the amount of prestress increases.

- In Figure 8, the experimental and finite element analysis results of the specimens, carrying maximum load of the 24a series, are given comparatively. In general, the maximum approximate values for the load carrying capacities are around 525 N and 6 mm for the G1-24a11 specimen. For other specimens it is determined that the maximum load carrying capacity decreases as the amount of prestress increases.

- In Figure 9, the experimental and finite element analysis results of the specimens, carrying maximum load of the 28a series, are given comparatively. In general, the maximum approximate values for the load carrying capacities are around 550 N and 4.5 mm for the G1-28a10 specimen.

It has been observed that there is an appropriate agreement between the results of the Force (N) - Displacement (mm) experimental data. The results of the finite element analysis obtained on the tensile tests applied on the structurally viscoelastic bonded specimens. Within the scope of our work, the maximum load carrying capacity specimens are identified. The detailed dimensional properties of these specimens are also given in Table 7.

Table 7. Dimensional properties of maximum load carrying capacity specimens.

Specimen		Prestress	c (mm)	d (mm)	b (mm)	a (mm)	Adhesive Area (mm^2)
16a Series	16a11	G1	16	11.2	40	40	448
	16a8	G2	16	9.6	40	40	384
	16a12	G3	16	11.2	48	40	448
	16a12	G4	16	11.2	48	40	448
20a Series	20a11	G1	20	14	40	40	560
	20a8	G2	20	12	40	40	480
	20a7	G3	20	12	32	40	480
	20a7	G4	20	12	32	40	480
24a Series	24a11	G1	24	16.8	40	40	672
	24a10	G2	24	16.8	32	40	672
	24a12	G3	24	16.8	48	40	672
	24a12	G4	24	16.8	48	40	672
28a Series	28a10	G1	28	19.6	32	40	784
	28a4	G2	28	14	32	40	560
	28a11	G3	28	19.6	40	40	784
	28a6	G4	28	14	48	40	560

Finally, according to the results obtained from the experimental and finite element analysis, it is determined that under the influence of different combined loads on viscoelastic VHB 4950 tape exhibits the maximum load carrying capacities specimens that low prestress and wide adhesion area. For a variety of applications, where variable loads are present, wide adhesion area should be preferred in order to achieve the best load carrying performance. Also, in order to have the best load carrying performance of the VHB 4950 tape, a minimum amount of prestressing should be applied.

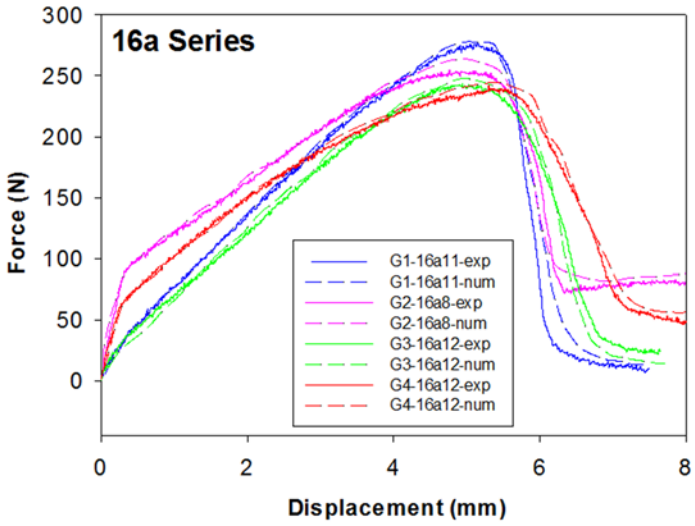

Figure 6. Maximum load carrying performances for 16a series

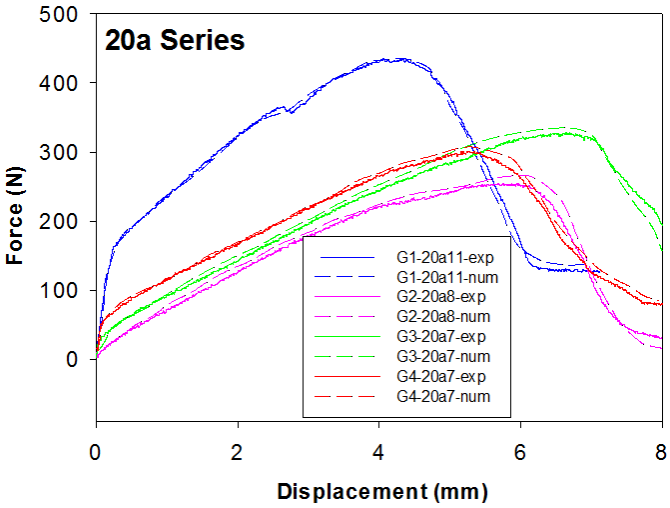

Figure 7. Maximum load carrying performances for 20a series

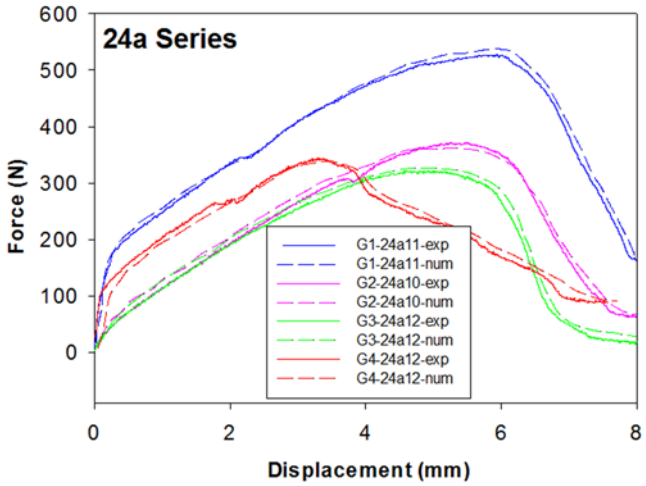

Figure 8. Maximum load carrying performances for 24a series

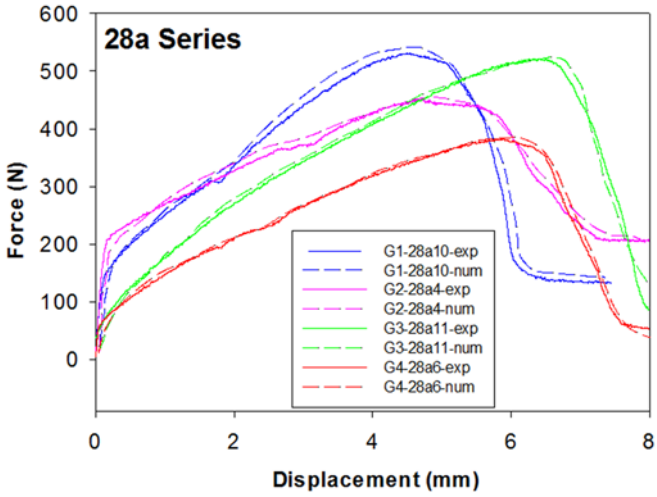

Figure 9. Maximum load carrying performances for 28a series

4. CONCLUSIONS

In this study, the mechanical behaviors of the VHB 4950 acrylic elastomer material used as adhesive tape under combined loads are investigated. For viscoelastic model, the experimental loading-unloading cyclic tests are carried out at different strain rates and at different stretch levels. Structurally specimens are performed under different prestressed. Thus, pre-stress effects on the maximum load carrying capacity of the structural specimens have also been investigated with experimental and finite element analysis. It has been determined that the most suitable material model is the Abaqus Parallel Rheological Framework Model 4 Yeoh Networks with Bergstrom-Boyce Flow model. In the future, the research of the maximum load carrying capacities under different temperature and humidity conditions can be carried out in the scope of this study. The specimen designs may be developed to provide different combined loads. In addition, the electro-active properties can be investigated by using pairs of different conductive and / or insulating materials instead of laminated composites used as structural constituents.

ACKNOWLEDGEMENTS

This work was financial supported by Research Fund of Uşak University. (Project Number: 2015/TP003)

REFERENCES

[1] Bergström JS, Boyce MC. Constitutive modeling of the large strain time-dependent behavior of elastomers. J Mech Phys Solids 1998; 46: 931-954.

[2] Johlitz M, Steeb H, Diebels S, Chatzouridou A, Batal J, Possart W. Experimental and theoretical investigation of nonlinear viscoelastic polyurethane systems. J Mater Sci 2007; 42: 9894–9904.

[3] Miehe C, Göktepe S, Lulei F. A micro-macro approach to rubber-like materials Part I: the non- affine micro-sphere model of rubber elasticity. J Mech Phys Solids 2004; 52: 2617-2660.

[4] Ask A, Menzel A, Ristinmaa M. Phenomenological modelling of viscous electrostrictive polymers. Int J Non-Linear Mech 2012; 47: 156-165.

[5] Vu DK, Steinmann P, Possart G. Numerical modelling of non-linear electroelasticity. Int J Numer Meth Engng 2007; 70: 685–704.

[6] Vu DK, Steinmann P. A 2-D coupled BEM–FEM simulation of electro-elastostatics at large strain. Comput Methods Appl Mech Engrg 2010; 199: 1124–1133.

[7] Büschel A, Klinkel S, Wagner W. A viscoelastic model for dielectric elastomers based on a continuum mechanical formulation and its finite element implementation. Proceedings SPIE 7976; Electroactive Polymer Actuators and Devices (EAPAD) 2011; 06 March 2011; San Diego, California, USA.

[8] Hossain M, Vu DK, Steinmann P. Experimental study and numerical modelling of VHB 4910 polymer. Comput Mat Sci 2012; 59: 65–74.

[9] Kaliske M, Rothert H. Formulation and implementation of three-dimensional viscoelasticity at small and finite strains. Comput Mech 1997; 19: 228–239.

[10] Nandi B, Dalrymple T, Yao J, Lapczyk I. Importance of capturing non-linear viscoelastic material behavior in tire rolling simulations. Meeting of the Tire Society; 8-10 September 2014; Providence, RI 02909, U.S.A.

[11] Wissler M, Mazza E. Mechanical behavior of an acrylic elastomer used in dielectric elastomer actuators. Sensors and Actuators A 2007; 134: 494–504.

[12] Vandenbroucke A, Laurent H, Aït Hocine N, Rio G. A hyperelasto-visco-hysteresis model for an elastomeric behaviour: Experimental and numerical investigations. Comput Mater Sci 2010; 48: 495–503.

[13] Amin AFMS, Lion A, Sekita S, Okui Y. Nonlinear dependence of viscosity in modeling the rate-dependent response of natural and high damping rubbers in compression and shear: Experimental identification and numerical verification. Int J Plast 2006; 22: 1610–1667.

[14] Johlitz M, Steeb H, Diebels S, Chatzouridou A, Batal J, Possart W. Experimental and theoretical investigation of nonlinear viscoelastic polyurethane systems. J Mater Sci 2007; 42: 9894-9904.

[15] Lion A. A physically based method to represent the thermo-mechanical behaviour of elastomers Acta Mech 1997; 123: 1–25.

[16] Wissler M, Mazza E. Modelling and simulation of dielectric elastomer actuators. Smart Mater Struct 2015; 14: 1396-1402.

[17] Mars, WV, Fatemi A. A novel specimen for investigating mechanical behavior of elastomers under multiaxial loading conditions, Experimental Mechanics 2004a; 44: 136–146.

[18] Qi HJ, Boyce MC. Constitutive model for stretch-induced softening of the stress-strain behavior of elastomeric materials. Journal Mech. Physics Solids 2004; 52: 2187-2205.

[19] Bergström JS, Rimnac CM, Kurtz SM. An augmented hybrid constitutive model for simulation of unloading and cyclic loading behavior of conventional and highly crosslinked UHMWPE. Biomaterials 2004; 25: 2171-2178.

[20] Yeoh, OH. Some forms of the strain energy function for rubber. Rubber Chem Technol 1993; 66: 754-771.

[21] PolyUMod Version 4.2.0 manual, A library of advanced user materials, Veryst Engineering.

[22] Gutierrez-Lemini D. Engineering viscoelasticity. New York, NY, USA: Springer Science+Business Media, 2014. pp. 113-145.

[23] Brinson HF, Brinson LC. Polymer engineering science and viscoelasticity, an introduction. 2nd ed. New York, NY, USA: Wiley, Springer Science+Business Media, 2015.

[24] Hurtado JA, Lapczyk I, Govindarajan SM. Parallel rheological framework to model non-linear viscoelasticity, permanent set, and Mullins effect in elastomers. Editors Gil-Negrete N, Alonso A, editors. Proceedings of the 8th European conference on constitutive models for rubbers; 25–28 June 2013; San Sebastián, Spain: Taylor & Francis Group, London, UK: ECCMR VIII pp. 95-100.

[25] Bergström JS. Constitutive modeling of elastomers—accuracy of predictions and numerical efficiency. PolymerFEM.com, 2005.

[26] 3M™ VHB™ Tapes Technical Data Sheet - October 2014.